

COLLISIONS AMONG CLOUDS INSIDE DUSTY TORUS IN ACTIVE GALACTIC NUCLEI: OBSERVATIONAL CONSEQUENCES

JIAN-MIN WANG

Laboratory for High Energy Astrophysics, Institute of High Energy Physics, CAS, Beijing 100039, P. R. China.

Received 2004 July 11; accepted 2004 August 25; published 2004 September 15

ABSTRACT

A geometrically thick dusty torus in NGC 1068 has been unambiguously resolved by an infrared interferometry telescope. This implies clouds composing the dusty torus are undergoing supersonic collisions with each other. We show that the collisions form strong non-relativistic shocks, which accelerate populations of relativistic electrons. Torus reprocesses emission from accretion disk into infrared band. We show that the energy density of the infrared photons inside the torus is much higher than that of the magnetic field in the clouds and the seed photons of inverse Compton scattering are mainly from the infrared ones. The maximum energy of the relativistic electrons can reach a Lorentz factor of 10^5 . We calculate the spectrum of the synchrotron and inverse Compton scattering radiation from the electrons in the torus. The relativistic electrons in the torus radiate non-thermal emission from radio to γ -ray, which isotropically diffuses in the region of the torus. We find the most prominent character is a peak at $\sim 0.5 - 1$ GeV. We apply this model to NGC 1068 and find that the observed radio emission from the core component S_1 can be explained by the synchrotron emission from the relativistic electrons. We predict that there is a γ -ray emission with a luminosity of 10^{40} erg/s peaking at ~ 1 GeV from the torus, which could be detected by *Gamma-Ray Large-Array Space Telescope* in the future. This will provide a new clue to understand the physics in the torus. The non-thermal radiation from dusty torus may explain the radio emission from Seyfert galaxies. The cosmological implications of the non-thermal emission to the γ -ray background radiation have been discussed.

Subject headings: galaxies: individual: NGC 1068; galaxies: nuclei

1. INTRODUCTION

A geometrically thick dusty torus has been recently resolved in the well-known Seyfert 2 galaxy NGC 1068 by an infrared interferometry telescope (Jaffe et al. 2004; hereafter). The dusty torus, as an essential ingredient in the unification scheme of active galactic nuclei (AGNs), plays a key role in obscuring the broad line region (Antonucci & Miller 1985; Antonucci 1993). How to maintain the thickness of the torus has long been puzzling in AGN physics. Krolik & Begelman (1988) suggested that the dusty torus is composed of discrete compressed clouds and supported by the random supersonic motion of clouds in z -direction. However, the inevitable collisions among the clouds dissipate their kinetic energy, an extra supply of kinetic energy to the clouds, such as a star cluster, is thus needed (Krolik & Begelman 1988; Jaffe et al. 2004). What are the observational consequences of the collisions?

VLBA (Very Long Baseline Array) has resolved the radio components in the core region of NGC 1068. The radio component S_1 at the center of the nucleus is coincident with the most powerful infrared source in NGC 1068 (Bock et al. 2000; Jaffe et al. 2004). The component S_1 should therefore relate to the dusty torus somehow physically. The inner edge of the hypothesized torus will be ionized by UV and X-rays from the accretion disk and is expected to be optically thick to free-free absorption at GHz frequencies (Neufeld et al. 1994). The free-free emission is suggested for the radio emission of the component S_1 from hot ionized gas of a temperature $T = 6 \times 10^6$ K and number density $n = 6 \times 10^5 \text{ cm}^{-3}$ evaporated from dust, and the inverted spectrum below 5GHz in NGC 1068 is explained by the ionized gas via free-free absorption with a total amount of $3400M_{\odot}$ (Gallimore et al. 2004). For typical values of the parameters, the ablation rate is of $\dot{M}_{\text{abl}} \approx 0.49M_{\odot} \text{ yr}^{-1}$ via photo-ionization (Krolik & Begelman 1988), the timescale for

the required mass of the ionized gas will be of $t_{\text{abl}} \approx 7 \times 10^3 \text{ yr}$. However, the free-free emission from hot ionized gas is proportional to the square of particle density and its cooling timescale is of, $t_{\text{ff}} \approx 3.2T_6^{1/2}n_6^{-1} \text{ yr}$, for the inferred ionized gas, where $T_6 = T/10^6 \text{ K}$ and $n_6 = n/10^6 \text{ cm}^{-3}$. It is clear that $t_{\text{ff}} \ll t_{\text{abl}}$, namely, most of the ionized gas ($\sim 3400M_{\odot}$) can not be maintained and will re-condense to dust. So there is no enough ionized gas to absorb the radio emission below 5 GHz in the model suggested by Gallimore et al. (2004). The fact that the Component S_1 nicely overlaps with the region of the most infrared bright torus (Jaffe et al. 2004) strongly implies that the radio emission from S_1 is linked with the torus itself. The explanation of this radio emission remains open. Does it relate to collisions among the clouds?

In this Letter, we focus on the observational consequences of the collisions among the clouds and show that shocks due to collisions accelerate populations of relativistic electrons. Non-thermal emission will be radiated as observational consequences from radio to GeV γ -rays. We apply this model to NGC 1068 and suggest that the radio emission of the component S_1 originates from the synchrotron emission of population of the relativistic electrons. The predicted γ -ray emission can be detected by *Gamma-ray Large-Array Space Telescope* (GLAST). This provides a new clue to test the mechanism supporting the torus.

2. NON-THERMAL EMISSION FROM TORUS

2.1. Cloud Collisions and acceleration of electrons

The detail micro-physics of clouds has been discussed by Krolik & Begelman (1988). The clouds are supported by self-gravity and magnetic field. Random motions of the clouds in the vertical direction support the thickness, $H_t \approx \Delta v / \Omega_K$, where H_t is the height of the torus, Δv is the random veloc-

ity in vertical direction and Ω_K is the Keplerian velocity of the clouds at the mid-plane. We then have $H_t/R_t \approx \Delta v/v_{\text{orb}}$, implying $\Delta v \sim v_{\text{orb}}$. It is expected that the clouds in torus are undergoing collisions in such a torus. The clumpy torus can be described by the clumpiness $\mathcal{C} = \Sigma_{\text{cl}}/\langle \Sigma_{\text{cl}} \rangle$, where Σ_{cl} and $\langle \Sigma_{\text{cl}} \rangle$ are the column density of each cloud and the mean column density of the torus, respectively. Genzel et al. (1985) estimate $\mathcal{C} \approx 0.1$ in the Galactic center. The total kinetic energy dissipated by the collisions for typical values of the parameters is given by Krolik & Begelman (1988)

$$\dot{E}_{\text{diss}} = 1.9 \times 10^{41} R_{\text{pc}} \Sigma_{25} \left(\frac{v_{\text{orb}}}{200 \text{ km/s}} \right)^3 \text{ (erg s}^{-1}\text{)}, \quad (1)$$

where the column density of the torus $\Sigma_{25} = \langle \Sigma_{\text{cl}} \rangle / 10^{25} \text{ cm}^{-2}$ and the distance to the black hole $R_{\text{pc}} = R_t / 1 \text{ pc}$. Part of this power is used to evaporate dust and left forms shocks which accelerate populations of relativistic electrons. We do not tackle the energy supply to the clouds in this paper.

The magnetic field in a cloud is expressed in term of the plasma parameter defined by $\beta = P_{\text{gas}}/P_{\text{mag}}$,

$$B = 1.3 \times 10^{-3} \beta_{0.2}^{-1/2} \mathcal{C}_{-1}^{1/2} \Sigma_{25}^{1/2} T_{300}^{1/2} \mathcal{H}^{-1/2} R_{\text{pc}}^{-1/2} \text{ (Gauss)}, \quad (2)$$

where $\mathcal{H} = H_t/R_t$, $\beta_{0.2} = \beta/0.2$, $\mathcal{C}_{-1} = \mathcal{C}/0.1$ and the temperature of the torus $T_{300} = T_t/300 \text{ K}$.

The Larmor gyration radius R_L of an electron with Lorentz factor γ_e is $R_L = 5.5 \times 10^{-8} (\gamma_5/B_{-3}) \text{ pc}$, where $\gamma_5 = \gamma_e/10^5$ and $B_{-3} = B/10^{-3} \text{ Gauss}$. This radius is much shorter than the size of the dusty torus. The temperature of the shocked gas during the collision is given by

$$T_s = \mathcal{M}^2 T_t \approx 1.2 \times 10^6 \Delta v_2^2 \text{ (K)}, \quad (3)$$

where March number $\mathcal{M} = \Delta v/v_{\text{th}}$, $\Delta v_2 = \Delta v/100 \text{ km s}^{-1}$ and $v_{\text{th}} = (kT_t/m_p)^{1/2}$ the sound speed. The shock velocity with respect to the unshocked gas v_{sh} are given by

$$v_{\text{sh}} = (\Gamma + 1) \left[\frac{kT_s}{(\Gamma - 1)m_p} \right]^{1/2} \approx 2.97 \times 10^7 T_6^{1/2} \text{ (cm s}^{-1}\text{)}, \quad (4)$$

where $\Gamma = 5/3$ is the adiabatic index, k the Boltzman constant, m_p the proton mass and $T_6 = T_s/10^6 \text{ K}$ the temperature of the shocked gas. The timescale of accelerating electrons reads (Blandford & Eichler 1987)

$$t_{\text{acc}} = \frac{R_L c}{v_{\text{sh}}} \approx 5.8 \times 10^7 \gamma_5 B_{-3}^{-1} T_6^{-1} \text{ (sec)}. \quad (5)$$

where c is the light speed.

The energy density of infrared photons inside the torus, which is reprocessed radiation from the accretion disk, can be estimated by

$$u_{\text{IR}} = \frac{L_{\text{IR}}}{2\pi^2 R_t^2 \mathcal{H} c} \approx 1.8 \times 10^{-5} L_{44} \mathcal{H}^{-1} R_{\text{pc}}^{-2} \text{ (erg cm}^{-3}\text{)}, \quad (6)$$

where $L_{44} = L_{\text{IR}}/10^{44} \text{ erg s}^{-1}$ is the infrared luminosity from the torus. We find $u_{\text{IR}} \gg u_B$, where u_B is energy density of the magnetic field. Thus the cooling of the relativistic electrons is mainly due to inverse Compton scattering of the infrared photons. The maximum energy of the electrons will be determined by the balances between the shock acceleration and the inverse Compton scattering of the IR photons inside the dusty torus. The timescale of energy loss due to inverse Compton (IC) scattering is given by

$$t_{\text{IC}} = \frac{3m_e c}{4\sigma_T \gamma_e u_{\text{IR}}} \approx 1.7 \times 10^8 \gamma_5^{-1} L_{44}^{-1} \mathcal{H} R_{\text{pc}}^2 \text{ (sec)}. \quad (7)$$

The maximum energy reaches when the acceleration timescale is equal to the IC timescale,

$$\gamma_{\text{max}} \approx 1.8 \times 10^5 L_{44}^{-1/2} \mathcal{H}^{1/2} R_{\text{pc}} B_{-3}^{1/2} T_6^{1/2}. \quad (8)$$

The shock acceleration is known to generally accelerate a power law distribution of relativistic electrons as $\gamma_e^{-\alpha}$, namely, the electron distribution function is

$$N(\gamma_e) = K \gamma_e^{-\alpha} = \frac{(3-\alpha)}{\gamma_{\text{max}}^{3-\alpha} - \gamma_{\text{min}}^{3-\alpha}} \frac{\xi_e \dot{E}_{\text{diss}}}{m_e c^2 c_0 u_{\text{IR}}} \gamma_e^{-\alpha}, \quad (9)$$

which follows from the energy equation that the relativistic electron is getting energy from the dissipation of the cloud collision

$$\int_{\gamma_{\text{min}}}^{\gamma_{\text{max}}} \dot{\gamma}_{\text{IC}} m_e c^2 N(\gamma_e) d\gamma_e = \xi_e \dot{E}_{\text{diss}}. \quad (10)$$

where $\dot{\gamma}_{\text{IC}} = c_0 u_{\text{IR}} \gamma_e^2$ ($c_0 = 3.2 \times 10^{-8} \text{ erg}^{-1} \text{ s}^{-1} \text{ cm}^{-3}$) is the energy loss rate of the electron due to inverse Compton scattering (Rybicki & Lightman 1979). Here ξ_e is the fraction of the thermal energy converted into the energy of the relativistic electrons.

2.2. Synchrotron Radiation and Inverse Compton Scattering

For a steady torus, the cloud collisions provide a constant energy supply to relativistic electrons. We have shown synchrotron losses of the electrons are much less than the inverse Compton scattering of the infrared photons. However the synchrotron radiation from the electrons is detectable in radio band as one observational consequence. The emergent spectrum from the torus will be given by the synchrotron and inverse Compton scattering emission. The peak frequency of the synchrotron emission is

$$\nu_{\text{syn}} \approx 4.2 \times 10^{13} B_{-3} \gamma_5^2 \text{ (Hz)}, \quad (11)$$

peaking at middle or near infrared band. This just overlaps with the peak frequency of the reprocessing of the disk and thus is under-detectable. We approximate the reprocessing of dusty torus as a black body with a single black body temperature of $T_{\text{eff}} = (L_{\text{IR}}/2\pi^2 a R_t^2 \mathcal{H} c)^{1/4} \approx 223 L_{44}^{1/4} \mathcal{H}^{-1/4} R_{\text{pc}}^{-1/2} \text{ K}$, where the black body radiation constant $a = 7.56 \times 10^{-15} \text{ erg cm}^{-3} \text{ deg}^{-4}$. The averaged energy of the infrared photons is $\epsilon_{\text{IR}} \approx 2.7 k T_{\text{eff}} \approx 5.2 \times 10^{-2} L_{44}^{1/4} \mathcal{H}^{-1/4} R_{\text{pc}}^{-1/2} \text{ eV}$ in torus, we have the peak of the inverse Compton scattering

$$\epsilon_\gamma \approx \gamma_{\text{max}}^2 \epsilon_{\text{IR}} \approx 0.52 \gamma_5^2 (\epsilon_{\text{IR}}/5.2 \times 10^{-2} \text{ eV}) \text{ (GeV)}. \quad (12)$$

We use the standard formulations of synchrotron and inverse Compton scattering including Klein-Nishina effects to calculate the spectra from torus for the typical values (Blumenthal & Gould 1970). The ratio of energy densities of magnetic field to synchrotron photons is of $u_B/u_{\text{ph}} \approx 10^{2\sim 3}$ for the typical values of the parameters, so self-Compton scattering emission can be neglected. Figure 1 shows the spectra for different electron index, but the injected energy $\xi_e \dot{E}_{\text{diss}}$ is fixed.

The synchrotron spectrum beyond radio band overlaps with the reprocessed emission from the torus itself. Since it is much lower than the later, this predicted component will be invisible or undistinguished. However, the component of $> 100 \text{ keV}$ spectrum will be observable because the overlapped continuum from disk/corona has a cutoff at 100 keV . This is a key feature of the present model. This component if detected only originates from the torus.

We emphasize that the non-thermal emission from torus is isotropic in the present model. The predicted spectra should be testable for any Seyfert galaxies as long as the dusty torus exists

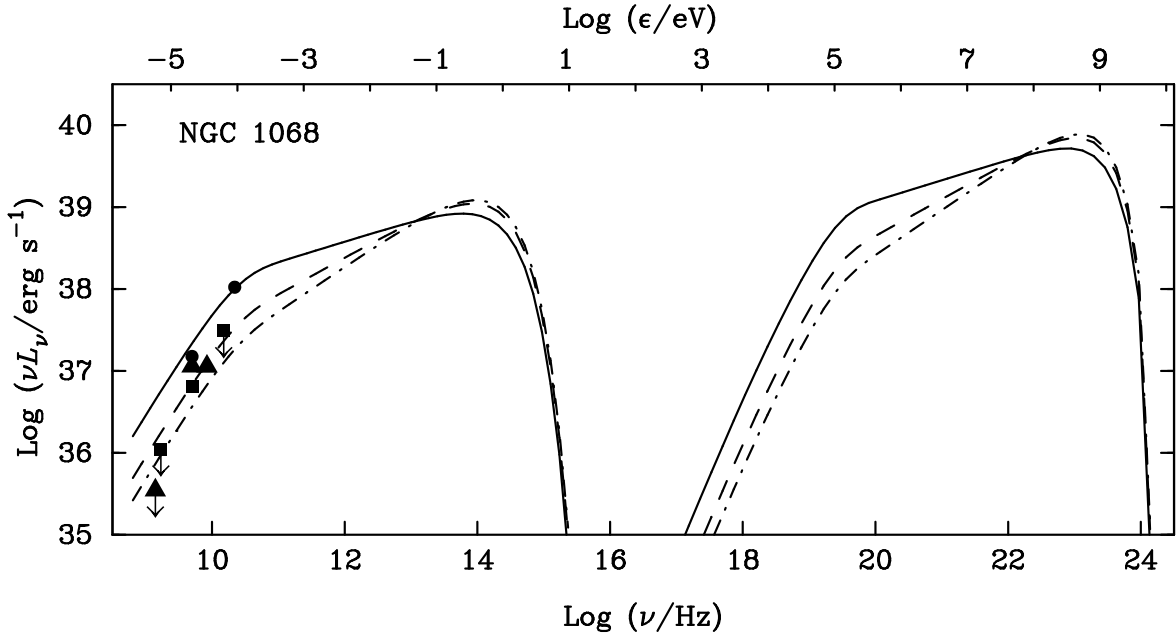


FIG. 1.— The spectrum of component S_1 . The parameter $\beta = 0.2$ is suggested in Krolik & Begelman (1988). We use the typical values of $B = 5 \times 10^{-3}$ Gauss, $\gamma_{\max} = 10^5$, $\gamma_{\min} = 900$, $u_{\text{IR}} = 10^{-5} \text{ erg cm}^{-3}$ and $\xi_e \dot{E}_{\text{diss}} = 3.0 \times 10^{40} \text{ erg/s}$. Spectral index α is taken for 2.5 (solid), 2.1 (dashed) and 1.9 (dash-dotted), respectively. There is a clear GeV bump predicted from the present model, which reaches a level detected by *GLAST*. The filled circles, squares and triangles are from Muxlow et al. (1996), Roy et al. (1998) and Gallimore et al. (2004). We note that the non-thermal emission from the torus is lower by a factor of $4 \sim 5$ orders than the emission from the central engine.

like in NGC 1068. In the present model, the soft X-ray emission lines are invisible since they are too faint compared with the soft X-ray spectrum of the nucleus. The model of Gallimore et al. (2004) predicts strong features in the soft X-ray band, but obscured by the torus itself in NGC 1068. It would be interesting to test the model suggested by Gallimore et al. (2004) in Seyfert 1 galaxies, which have dusty tori and the predicted luminous soft X-ray emission lines unobscured by the tori will be viewed by *Chandra*. The present model does not depend on the types of Seyfert galaxies provided there are geometrically thick tori in these objects. So it is not difficult to distinguish the two different models in principle.

3. APPLICATION TO NGC 1068

The amount of the ionized gas can be estimated from the balance between the free-free cooling and the ablation of dust in the torus. The ablation timescale is $t_{\text{abl}} = M_{\text{gas}}/\dot{M}_{\text{abl}}$, where the mass of the ionized gas is $M_{\text{gas}} \approx 2\pi^2 n_{\text{th}} m_p \mathcal{H}^2 R_t^3$ and n_{th} the number density of the ionized gas. We then have $n_{\text{th}} \approx 1.1 \times 10^4 T_6^{1/4} \mathcal{H}^{-1} R_{\text{pc}}^{-3/2}$ (cm^{-3}) from $t_{\text{abl}} = t_{\text{ff}}$. The optical depth of free-free absorption of the ionized gas is $\tau_{\text{ff}} = 1.4 \times 10^{-3} T_6^{-3/2} \nu_{\text{GHz}}^{-2} n_4^2 R_{\text{pc}}$, where $\nu_{\text{GHz}} = \nu/10^9 \text{ Hz}$ and $n_4 = n_{\text{th}}/10^4 \text{ cm}^{-3}$. It is thus impossible for free-free absorption to cause an invert spectrum at $\sim \text{GHz}$. The free-free emission from the ionized gas is of $5.3 \times 10^{32} n_4^2 T_6^{-1/2} \nu_{\text{GHz}} \mathcal{H}^2 R_{\text{pc}}^3$ (erg s^{-1}), much lower than synchrotron radiation from the relativistic electrons. Here the Gaunt factor is neglected in our estimations. The thermal electrons from the evaporation has a Thomson scattering depth of $\tau_{\text{es}} = 2.0 \times 10^{-2} n_4 R_{\text{pc}}$. This value is consistent with the fraction of the polarized emission to the total due to the thermal electrons (Antounucci & Miller 1985). Additionally the free-free emission gets a peak flux of 10^{38} erg/s at $\sim 0.1 \text{ keV}$, which is overwhelmed by the radiation from the

core. We can not detect such a faint radiation component.

The Eddington ratio is roughly $L_{\text{Bol}}/L_{\text{Edd}} \sim 0.44$, where the mass of the black hole $M_{\text{BH}} = 10^{7.23} M_{\odot}$ estimated from maser observation (Greenhill et al. 1997) and the bolometric luminosity $L_{\text{Bol}} = 10^{44.98} \text{ erg/s}$ by integrating the multiwavelength continuum (Woo & Urry 2002). It is much higher than the critical accretion rate of advection-dominated accretion flow (ADAF). This indicates that the radio emission from the Component S_1 can not originate from an optically thin ADAF in NGC 1068. Roy et al. (1998) suggested that the component S_1 may originate from synchrotron radiation from the relativistic electrons, but it remains open how to accelerate electrons.

TABLE 1 FUTURE OBSERVATIONS

| Instrument | Energy Band | Threshold (photons $\text{cm}^{-2} \text{ s}^{-1}$) | Note |
|------------------------------------|---------------|---|------|
| <i>INTEGRAL</i> /SPI ¹ | 20 keV-8 MeV | 2.4×10^{-3} @8MeV | × |
| <i>INTEGRAL</i> /IBIS ¹ | 20 keV-10 MeV | 5.0×10^{-5} @10MeV | × |
| <i>GLAST</i> ² | > 100 MeV | 1.6×10^{-9} | ✓ |
| <i>Agile</i> ³ | 30MeV-50GeV | 5.0×10^{-8} @1 GeV | ? |

¹<http://astro.estec.esa.nl/SA-general/Projects/Integral>

²<http://www-glast.stanford.edu/mission.html>

³<http://agile.mi.iasf.cnr.it/Homepage/performances.shtml>

We use the typical values of the parameters in the present model. The dissipation rate of the kinetic energy via cloud collisions is $\dot{E} \approx 2.0 \times 10^{41} \text{ erg/s}$, and $\xi_e = 0.15$. The radiation luminosity via inverse Compton scattering is of $\sim 10^{40} \text{ erg/s}$. We find that the radio spectrum of S_1 can be generally fitted by synchrotron emission. The most prominent character in Figure 1 is the GeV bump, which is caused by inverse Compton scattering of the infrared photons inside the torus. This bump corresponds to a flux of $\sim 10^{-9}$ photons $\text{cm}^{-2} \text{ s}^{-1}$ at 1 GeV and $\sim 10^{-8}$ photons $\text{cm}^{-2} \text{ s}^{-1}$ at $> 100 \text{ MeV}$. Detection of this component is essential to probe physics inside the torus.

Seyfert galaxies have been observed by *EGRET*, showing up-

per limit with 2σ (Lin et al. 1993). Table 1 lists the sensitivities of several missions. The last column gives the comments to observations. We find that the Italian mission *Agile* could marginally detect GeV bump in NGC 1068 and *GLAST* has capability of detecting this GeV bump.

The synchrotron self-absorption (SSA) depth is numerically given by $\tau_{\text{syn}} \approx 1.5 \times 10^{-5} K_{56} R_{\text{pc}}^{-2}$ ($\alpha = 2.5$, $\gamma_{\text{min}} = 900$, $B = 5.0 \times 10^{-3}$ Gauss) at 1 GHz, where $K_{56} = K/10^{56}$, for a spatially homogeneous distribution of the relativistic electrons inside the torus. This shows less importance of the SSA, however we note that this may severely underestimate τ_{syn} depending on the spatial density distribution of the electrons. This is because we use the number density of the relativistic electrons averaged over the entire torus, which is much lower than the local. Additionally, the GHz spectrum may rely on the break energy of the electron distribution, which is determined by the detail of processes of the acceleration and cooling. We remain it as a free parameter to fit the spectrum since we pay main attention to the observational consequences of cloud collisions. Future detail numerical simulations of cloud collisions may display some details of accelerations so that the minimum energy of the electrons and SSA depth will be given.

4. DISCUSSIONS

Collisions simultaneously lead to loss of angular momentum of molecular clouds and then determine the accretion rate of the black hole (Krolik & Begelman 1988). Therefore the present model predicts a strong correlation between the radio emission from torus and a parameter representing the accretion rate. Indeed Ulvestad & Ho (2001) find a very strong correlation, $P_{6\text{cm}} \propto L_{[\text{O III}]}^{1.5}$ (estimated from their Fig 5) in the Palomar Seyfert galaxies, where $L_{[\text{O III}]}$ is the [O III] luminosity and $P_{6\text{cm}}$ is the radio emission power at 6cm. $L_{[\text{O III}]}$ is a good indicator of the accretion rate of the black hole since $L_{[\text{O III}]} \propto L_{\text{ion}}$, where L_{ion} is the ionizing luminosity. We note that the collisions lead to angular momentum loss of clouds, which will be accreted onto the black hole. Therefore the radio emission and $L_{[\text{O III}]}$ are related with the physics of cloud collisions. The $P_{6\text{cm}} - L_{[\text{O III}]}$

correlation could be explained by the present model. The predicted radio flux in the present model depends on electron index α , a more careful study on this will be carried out in future.

The isotropic radiation of the relativistic electrons may imply a significant contribution to the γ -ray background radiation. If the typical γ -ray luminosity from torus is of $L_{\gamma}^{\text{AGN}} \approx 10^{40}$ erg/s, we have the contributed flux to the γ -ray background radiation $F_{\gamma} \approx \phi_{\text{AGN}} L_{\gamma}^{\text{AGN}} \Delta V / 4\pi d_L^2$, where ϕ_{AGN} is AGN number density peak, ΔV is the shell volume of the AGN number peak at redshift $z \approx 1$ and d_L is the distance the peak shell. We have the contribution of AGN torus to the γ -ray background $F_{\gamma} \approx 0.6 \text{ keV cm}^{-2} \text{ s}^{-1} \text{ sr}^{-1}$ for $\phi_{\text{AGN}} = 5.0 \times 10^{-5} \text{ Mpc}^{-3}$ from X-ray observation (Steffen et al. 2003) and the peak shell width $\Delta R \approx d_L$. The deduced γ -ray background emission is of $1.0 \text{ keV cm}^{-2} \text{ s}^{-1} \text{ sr}^{-1}$ below 1 GeV (see Figure 1 in Loeb & Waxman 2000). The predicted GeV flux significantly contributes to background emission below 1 GeV. It is interesting to note that the background emission spectrum shows increases below 0.6 GeV (Loeb & Waxman 2000). It is worth investigating this subject in detail further.

5. CONCLUSIONS

We suggest that the collisions among the clouds inside the torus produce populations of relativistic electrons in active galactic nuclei. Non-thermal emission from relativistic electrons is detectable in radio and γ -ray band. The radio emission from the Component S_1 in NGC 1068 can be explained by the present model. It is predicted that there is a GeV bump in NGC 1068, which is caused by inverse Compton scattering off the infrared photons inside dusty torus. This GeV component can be detected by *GLAST*. We also show that the GeV bump of radiation from torus could significantly contribute to the background radiation of < 1 GeV.

I thank the anonymous referee for the helpful and prompt comments. This research is supported by Grant for Distinguished Young Scientists from NSFC, Hundred Talent Program of CAS and 973 project.

REFERENCES

- Antonucci, R.R.J., 1993, ARA&A, 31, 473
 Antonucci, R.R.J. & Miller, J.S., 1985, ApJ, 297, 621
 Blandford, R. & Eichler, D., 1987, Phys. Rep., 154, 1
 Blumenthal, G.R. & Gould, R.J., 1970, Rev. Mod. Phys., 42, 237
 Bock, J.J., et al., 2000, AJ, 120, 2904
 Gallimore, J.F., Baum, S.A. & O'Dean, C.P., 2004, ApJ, in press.
 Genzel, R., Watson, D.M., Crawford, M.K. & Townes, C.H., 1985, ApJ, 297, 766
 Greenhill, L.J., Moran, J.M. & Herrnstein, J.R., 1997, ApJ, 481, L23
 Jaffe, W., et al., 2004, Nature, 429, 471
 Krolik, J.H. & Begelman, M.C., 1988, ApJ, 329, 702
 Lin, Y.C., et al., 1993, ApJ, 416, L53
 Loeb, A. & Waxman, E., 2000, Nature, 405, 156
 Muxlow, T.W., et al. 1996, MNRAS, 278, 854
 Neufeld, D.A., Maloney, P.R. & Conger, S., 1994, ApJ, 436, L127
 Roy, A.L., Colbert, E.J.M., Wilson, A.S., & Ulvestad, J.S., 1998, ApJ, 504, 147
 Rybicki, G.B. & Lightman, A.P. 1979, Radiative Processes in Astrophysics, John Wiley & Sons (New York)
 Steffen, A.T. et al., 2003, ApJ, 596, L23
 Ulvestad, J.S. & Ho, L.C., 2001, ApJ, 558, 561
 Woo, J.H. & Urry, C.M., 2002, ApJ, 579, 530